ELSEVIER

Earth and Planetary Science Letters 150 (1997) 27–39

EPSL

Prolonged residence times for the youngest rhyolites associated with Long Valley Caldera: $^{230}Th-^{238}U$ ion microprobe dating of young zircons

Mary R. Reid [*,1], Christopher D. Coath, T. Mark Harrison, Kevin D. McKeegan

W.M. Keck Foundation Center for Isotope Geochemistry, Department of Earth and Space Sciences and IGPP, University of California, Los Angeles, CA 90095-1567, USA

Received 24 October 1996; revised 21 April 1997; accepted 26 April 1997

Abstract

We describe a new ion microprobe method for dating magmatic zircon growth that is based on in situ measurement of the magnitude of $^{238}U-^{230}Th$ disequilibrium. Our results support independent inferences that zircon can remain suspended for long periods (> 100 ka) in the convecting portions of the magma from which it crystallizes. Because the crystallization ages date when the magma cooled to its zircon saturation temperature, even when the zircons have long magmatic residence times, $^{238}U-^{230}Th$ zircon dating can be used to constrain the thermochemical evolution of silicic magmas.

$^{238}U-^{230}Th$ ages have been determined for individual zircons from rhyolites associated with the Long Valley magmatic system of eastern California. The samples are from Deer Mountain, an 115 ± 3 ka low-silica moat rhyolite, and from the coarsely porphyritic, low-silica rhyolite of South Deadman dome, one of the ~0.6 ka Inyo domes. Previous investigations have suggested that the two lavas were derived from the same magma reservoir. A few of the zircon model ages, calculated with respect to the isotopic characteristics of the whole rocks, are within error of that for eruption of the Deer Mountain rhyolite. However, the majority of zircons from both lavas cluster around an age of ~230 ka. This common interval of zircon nucleation and growth, for petrologically similar lavas, suggests that the younger Inyo dome lava may have tapped the same magma body from which the Deer Mountain rhyolite erupted more than 100 ka before. On the other hand, most of the zircon model ages are younger than previous episodes of silicic volcanism in the Long Valley Caldera, suggesting that the rhyolites may have been generated during development of a silicic upper crustal magma chamber in the western portion of Long Valley caldera. Zircon saturation temperatures for the rhyolites studied (795–810°C) are the same as those obtained from coexisting Fe–Ti oxides (809 ± 4°C), showing that the magma cooled to < 815°C more than 200 ka ago. The surprising consequence of these temperatures is the apparent longevity of the shallow magma reservoir from which relatively small (< 1 km^3) volume magmas erupted. The magma reservoir could have remained molten because of the regular influx and differentiation of mafic magma, resulting in accumulation of a much larger volume of magma than that erupted.

Keywords: Long Valley Caldera; residence time; zircon; U-238/Th-230; ion probe data; rhyolites

* Corresponding author. Tel.: +1 310 825 1756. Fax: +1 310 825 2779. E-mail: reid@ess.ucla.edu

[1] Also affiliated with: White Mountain Research Station, 3000 East Line Street, Bishop, CA 93514, USA.

0012-821X/97/$17.00
PII S0012-821X(97)00077-0

1. Introduction

The frequent occurrence of zircon as an inclusion in major phenocryst phases in rhyolites and rhyodacites shows that the thermochemical conditions for zircon crystallization may be reached prior to eruption, during magmatic differentiation. Provided they remain suspended, zircons grown in this fashion may have quantifiable magmatic residence times. Several features of zircon make it amenable to dating on short time-scales by Th isotope analyses. First, U is concentrated preferentially with respect to Th during crystallization of zircon [1,2], resulting in significant excess of ^{238}U over its daughter ^{230}Th. Subsequent ingrowth of ^{230}Th ($t_{1/2} = 75$ ka) in response to this U enrichment provides a means of determining the time that has elapsed since crystallization occurred. The five-fold or greater U enrichment ([1]; this study) is sufficiently large that ages determined in this fashion are relatively insensitive to assumptions about the initial ^{230}Th content of the zircon. Further, the slow diffusion of U and Th in zircon [3] should result in preservation of U–Th crystallization ages, even at magmatic temperatures. When combined with the temperature dependence of zircon saturation [4,5], zircon crystallization ages offer important opportunities for gaining insights into magmatic evolution.

In this paper, we report the first in situ Th isotope analyses of zircon. Ion microprobe analyses permit dating of subdomains within individual zircons grains and thus provide a means of obtaining a potentially continuous record of the thermochemical evolution of the magma reservoir, including recognition of multiple episodes of crystallization and of xenocrysts diagnostic of crustal assimilation. We have applied this technique to two lavas that erupted near the western margin of the Long Valley Caldera of eastern California (Fig. 1): Deer Mountain, a 115 ± 3 ka low-silica moat rhyolite [6], and the coarsely porphyritic low-silica rhyolite of South Deadman Dome, one of the ~ 0.6 ka Inyo domes [7]. These lavas were chosen because they are relatively young, contain large zircons (> 50 μm), and have been proposed to originate in the same magma reservoir [8,9]. They are among the latest manifestations of the protracted effusive silicic volcanism (> 2 Ma; [10]) on the eastern flank of the Sierra Nevada which was punctuated at 0.76 Ma [11] by catastrophic eruption of the Bishop Tuff and caldera collapse. Long (0.3–1.1 Ma) magmatic residence times have been inferred for silicic precaldera and caldera-forming lavas based on whole-rock [12] and mineral [13,14] ^{87}Rb–^{86}Sr isochrons and on $^{40}Ar/^{39}Ar$ and ^{87}Rb–^{86}Sr dating of glass inclusion-bearing quartz phenocrysts [15,16]. Our ion microprobe Th isotope analyses provide further insight into the evolution of silicic magmas because we can detect mixed mineral populations and examine their age distributions. Once the magmatic age is defined, we can use this information in conjunction with the temperature-dependence of zircon precipitation to place a constraint on the thermal evolution of the rhyolitic magmas. We conclude that, despite having small eruption volumes and erupting more than 100 ka apart, the lavas studied here are likely derived from a common silicic magma reservoir that cooled to a temperature of

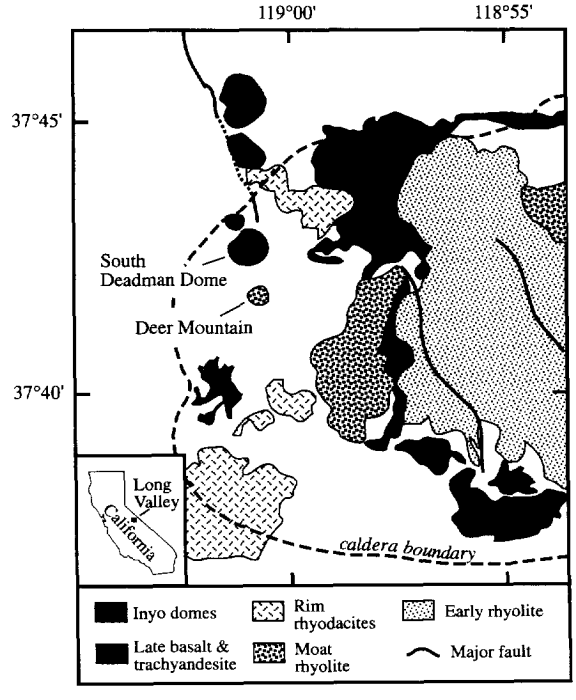

Fig. 1. Simplified geologic map of the western part of Long Valley Caldera showing the locations of Deer Mountain and South Deadman Dome, the rhyolites studied. The map is based on [17] and shows the distribution of major postcaldera volcanic units within the caldera, including the early rhyolites, moat rhyolites, and rim rhyodacites. The topographic boundary of Long Valley Caldera and inferred ring fault are also shown.

< 815°C more than 200 ka ago. As for the pre-caldera and caldera-forming rhyolites, heat loss from the magma body appears to have been balanced by basaltic influx in a way that maintained supersolidus conditions for long periods of time.

2. Geologic setting and sample descriptions

The zircons studied here are those of coarsely porphyritic lavas from the western margin of Long Valley Caldera. Lavas exposed in this area erupted from 260 to < 1 ka [6] and range in composition from trachybasalts to high-silica rhyolite [17]. Although generally considered to be post-caldera in origin, this late Quaternary magmatic activity transects the caldera in a roughly N–S direction and extends well to the north of it. Deer Mountain is one of four 'moat' rhyolites of ~ 110 ka age (Fig. 1) that erupted after more than 300 m of mafic to intermediate lavas infilled the western moat of the caldera [18,19]. South Deadman Dome is one of three large silicic domes associated with the Inyo volcanic chain (Fig. 1), which terminates to the south at phreatic explosion craters on the summit and south flank of Deer Mountain [7,8]. It is texturally bimodal at a megascopic scale [8,20], consisting of finely and coarsely porphyritic phases. The latter composes the core of the dome, a distribution that may reflect draw-up of the coarsely porphyritic magma from a compositionally stratified dike system or zonal segregation in the conduit as a result of contrasting viscosities [21,22]. The total volume of coarsely porphyritic lavas erupted in the Inyo domes is probably < 1 km^3 (cf. [7,20,21]).

The Deer Mountain rhyolite is compositionally similar but slightly more evolved than the average coarsely porphyritic Inyo dome lava (data of [9,18]). Both lavas contain the following phenocryst assemblage: plagioclase > sanidine > biotite > hornblende > quartz > Fe–Ti-oxides > orthopyroxene + clinopyroxene + zircon ± allanite, but the older lava is somewhat less phenocryst-rich than the Inyo domes coarsely porphyritic lavas (25–40 vol% phenocrysts; [9]). Compositional and petrographic similarity between these two lavas has been attributed to their derivation from a common magma body [8,9]. Based on the location of these lavas on or inside the present-day caldera walls, their source has been inferred to lie beneath the caldera itself. However, the absence of Bishop Tuff in a drill core located just to the south of Deer Mountain [18] may indicate that the domes actually vented outside of the caldera ring fractures (Fig. 1). The phenocryst assemblage of these lavas is stable in magmas with water contents of > 4 wt% and temperatures of less than ~ 835°C [23,24]. Aluminum solubility in hornblende further suggests that the coarsely porphyritic Inyo dome lavas may have equilibrated at upper crustal depths [22]. These conditions are broadly consistent with those inferred from a variety of geophysical measurements ([25–27] and references therein) for a low-velocity, low density anomaly beneath the western half of the caldera.

3. $^{230}Th/^{238}U$ ion microprobe dating of zircon

^{238}U decays to ^{206}Pb through a series of shorter-lived radionuclides, the longest lived of which are ^{234}U ($t_{1/2}$ = 246 ka) and its daughter ^{230}Th ($t_{1/2}$ = 75 ka). In most igneous rocks [28], and therefore their zircons, the activities of ^{238}U and ^{234}U are equal, a condition known as secular equilibrium, and ^{238}U can be used as a proxy for ^{234}U. Zircon preferentially concentrates U such that the initial $^{230}Th/^{238}U$ of zircon is low. $^{230}Th/^{238}U$ subsequently increases in response to the decay of ^{238}U but, because ^{230}Th is also radioactive, the rate of increase is dictated largely by the rate of ^{230}Th decay. The abundance of ^{230}Th in a young zircon will cease to change when ^{230}Th and ^{238}U are in secular equilibrium, wherein the $^{230}Th/^{238}U$ atom ratio is equal to the ratio of their half-lives (1.687×10^{-5}). Some ^{230}Th is also incorporated by zircon initially, and the magnitude of this 'common' ^{230}Th can be evaluated from the ^{232}Th content if the initial $^{230}Th/^{232}Th$ of zircon is known or can be inferred. In this study, the zircons are assumed to have the same initial $^{230}Th/^{232}Th$ as the host whole rocks in which they are contained. Our results show that initial $^{230}Th/^{238}U$ ratios of zircon are sufficiently low so that Th isotope ages are relatively insensitive to uncertainties in the initial $^{230}Th/^{232}Th$ of the zircon.

Atomic ratios between ^{238}U, ^{230}Th, and ^{232}Th in zircons were analyzed using a CAMECA ims 1270

Table 1
U–Th isotope data for South Deadman Dome and Deer Mountain zircons and whole rocks

	UO (10^4 cps)	$\frac{(^{230}Th)}{(^{232}Th)}$ [a]	±	$\frac{(^{238}U)}{(^{232}Th)}$ [a]	±	$\frac{(^{230}Th)}{(^{238}U)}$ [a]	±	Model age [b] (ka)	+	−
South Deadman Dome										
92LV08 whole rock [c]		0.928	0.002	0.930		0.998				
92LV08 zircons (80–270 mesh) [d]										
LV08gr4sp1r	8.45	2.96	0.11	3.463	0.009	0.85	0.03	177	26	21
LV08gr4sp2c	2.83	3.43	0.23	4.114	0.014	0.84	0.06	168	45	32
LV08gr6sp1	20.2	1.47	0.05	3.170	0.002	0.46	0.02	30	3	3
LV08gr7sp1r	6.74	10.66	1.32	10.602	0.097	1.01	0.12	–	–	–
LV08gr7sp2r	6.57	10.26	0.49	12.577	0.027	0.82	0.04	176	26	21
LV08gr9sp1r	3.09	5.33	0.32	7.751	0.045	0.69	0.04	113	16	14
LV08gr9sp2c	3.20	5.22	0.34	6.764	0.064	0.77	0.05	144	28	22
LV08gr10sp1	6.89	4.29	0.19	4.796	0.055	0.90	0.04	221	53	36
LV08gr15sp1	8.44	5.55	0.22	5.972	0.008	0.93	0.04	271	79	45
LV08gr16sp1	12.7	9.16	0.28	10.208	0.011	0.90	0.03	237	35	26
LV08gr17sp1r	20.0	3.93	0.08	4.250	0.014	0.93	0.02	255	31	24
LV08gr17sp2c	6.90	6.86	0.27	7.566	0.013	0.91	0.04	243	51	35
LV08gr19sp1	5.89	4.63	0.22	5.432	0.008	0.85	0.04	188	35	26
LV08gr23sp1	2.48	3.85	0.25	4.096	0.008	0.94	0.06	278	–	202
Deer Mountain										
92LV05 whole rock [c]		0.939	0.002	0.983		0.955				
92LV05 zircons (80–400 mesh) [d]										
LV05-1gr3sp1	7.73	4.64	0.50	5.861	0.044	0.79	0.08	155	61	39
LV05-1gr4sp1	17.2	7.65	0.48	7.862	0.014	0.97	0.06	405	–	148
LV05-1gr4sp2	4.94	8.54	0.36	9.981	0.013	0.86	0.04	203	32	25
LV05-1gr5sp1	14.6	5.90	0.13	6.509	0.023	0.91	0.02	248	29	23
LV05-2gr1sp1	14.7	4.63	0.16	6.506	0.075	0.71	0.02	120	10	9
LV05-2gr2sp1	33.8	4.24	0.10	4.982	0.003	0.85	0.02	190	16	14
LV05-2gr3sp1	5.55	4.77	0.20	5.150	0.004	0.93	0.04	275	101	51
LV05-2gr4sp1	11.8	3.97	0.13	4.256	0.004	0.93	0.03	285	89	48
LV05-2gr9sp1c	15.2	9.27	0.24	9.284	0.008	1.00	0.03	–	–	–
LV05-2gr9sp2r	11.5	7.74	0.24	8.010	0.010	0.97	0.03	375	–	79
LV05-2gr11sp1	10.7	4.29	0.14	4.657	0.026	0.92	0.03	264	61	39
LV05-2gr24sp1r	13.7	7.61	0.25	9.090	0.011	0.84	0.03	188	21	17
LV05-2gr24sp2c	11.2	4.58	0.18	5.057	0.021	0.91	0.04	245	60	38
LV05-2gr25sp1	15.9	7.23	0.23	7.984	0.007	0.91	0.03	249	42	30
LV05-2gr27sp1r	9.58	4.56	0.17	6.401	0.006	0.71	0.03	120	11	10
LV05-2gr27sp2c	10.6	4.83	0.19	6.274	0.024	0.77	0.03	145	16	14
LV05-2gr29sp1r	6.94	6.53	0.27	7.354	0.013	0.89	0.04	229	46	32
LV05-2gr29sp2r	20.2	3.57	0.06	4.047	0.007	0.88	0.02	213	17	15

[a] Activity ratios calculated from isotopic ratios using the following decay constants: $\lambda_{232} = 4.9475 \times 10^{-11}$ y^{-1}; $\lambda_{230} = 9.1952 \times 10^{-6}$ y^{-1}; $\lambda_{238} = 1.55125 \times 10^{-10}$ y^{-1}.

[b] Model ages calculated from two-point zircon–whole rock isochrons; uncertainties are 1σ. ^{234}U is assumed to be in secular equilibrium with ^{238}U, by analogy to other magmas [28].

[c] Whole-rock analyses performed by thermal ionization mass spectrometry as in [29]; reported errors are 2σ; reproducibility is $< 1\%$ for $(^{230}Th)/(^{232}Th)$ and $< 1.5\%$ for $(^{238}U)/(^{232}Th)$.

[d] Zircon analyses are reported by grain (gr) and spot (sp) number and, where duplicate analyses were performed, by relative proximity to rim (r) or core (c). Note that zircons identified as LV08, LV05-1, and LV05-2 were run in different sessions, such that differences in $^{238}U^{16}O$ beam intensities between grains analyzed in different sessions may reflect different running conditions rather than differences in actual U content.

high resolution ion microprobe. Whole-rock $^{238}U/^{232}Th$ and $^{230}Th/^{232}Th$ atom ratios were obtained by thermal ionization mass spectrometry following standard procedures [29]. For the ion microprobe measurements, primary beam currents of 5–10 nA were focused on Au-coated, highly polished zircons mounted in epoxy. Analyzed sputtered areas varied from 400 to 700 μm^2. Analyses were performed using an $^{16}O^-$ primary ion beam; experiments with O_2^- primary beam yielded stable secondary ion beams that were of lower intensity than those of O^-. As secondary ion yields of ThO^+ and UO^+ were greater than those for the elemental ions, we calibrated the oxide ions to determine Th/U ratios. $^{230}Th^{16}O$ has two isobaric interferences on the low mass side. These interferences were well resolved at a mass resolution of 4400 (full width at 10% of maximum) and there was no detectable change in $^{230}Th^{16}O^+/^{238}U^{16}O^+$ when the mass resolving power (MRP) was increased to 6500. Unresolved molecular interferences with $^{230}Th^{16}O$ at a MRP above 4400 are unlikely: ^{230}Th has a positive mass defect whereas molecules with the same mass number will be formed of less massive nuclides which, except for the lightest stable nuclides (< 15 amu), have negative mass defects. Typical $^{238}U^{16}O^+$ intensities attained in this study ranged from 10^4 to 10^5 counts per second (cps; Table 1); $^{230}Th^{16}O^+$ intensities ranged from 0.4 to 5 cps. Average background counting rates during the analyses were 0.04 $\pm$ 0.01 cps and measured $^{230}Th^{16}O$ peaks were corrected for this contribution.

ThO^+ and UO^+ have different ionization yields during sputtering, such that a correction factor must be applied to measured $^{230}Th^{16}O^+/^{238}U^{16}O^+$ and $^{232}Th^{16}O^+/^{238}U^{16}O^+$. Most zircons, even highly concordant ones (e.g., [30]), are heterogeneous with respect to Th/U; those that are relatively homogeneous with respect to actinides (e.g., Mud Tank carbonatite; [31]) are typically characterized by very low Th and U concentrations. We circumvented the need for a homogeneous zircon standard by calibrating Th/U correction factors against the internal isotopic characteristics of old, concordant zircons. The zircons used are from the 1.1 Ga anorthositic series of the Duluth Complex, taken from the same locality as sample AS3 [32]. These zircons yield highly concordant $^{238}U-^{206}Pb$, $^{235}U-^{207}Pb$, and $^{232}Th-^{208}Pb$ ages. Pb isotope analyses were performed, following techniques described in [33], at the same time as ThO^+/UO^+ measurements. Radiogenic Pb, $^{208}Pb^*/^{206}Pb^*$, is strongly correlated with measured $^{232}Th^{16}O^+/^{238}U^{16}O^+$ (Fig. 2). The ThO^+/UO^+ relative sensitivity factor, obtained from the difference between the measured slope and that anticipated for 1.1 Ga Pb isotope in-growth, is 1.080 $\pm$ 0.008 (1σ).

Ratios of $^{230}Th^{16}O^+/^{238}U^{16}O^+$ were also measured in the Duluth Complex zircons. ^{238}U and ^{230}Th activities in these zircons should be at secular equilibrium, and therefore, after the Th/U correction factor is applied, the calculated activities of ^{230}Th

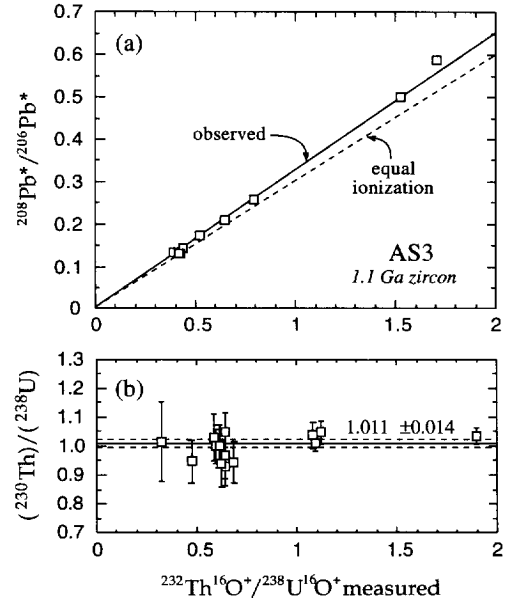

Fig. 2. (a) Ratio of radiogenic ^{208}Pb to ^{206}Pb ($^{208}Pb^*/^{206}Pb^*$) versus measured $^{232}ThO^+/^{238}UO^+$ in 1.1 Ga zircon standard AS3; Pb isotope ratios are corrected for common Pb using the initial ratios of [32]. The highly concordant nature of the U–Pb and Th–Pb systems in this zircon allows a relative sensitivity factor to be calculated for converting ion yields of ThO^+ and UO^+ into atomic ratios of ^{232}Th and ^{238}U. The predicted correlation for equal ionization of ThO^+ and UO^+ has a slope of 0.3006; a least-squares fit to the data yields a slope of 0.3248 $\pm$ 0.0023 and an intercept of 0.0010 $\pm$ 0.0017 (MSWD = 2.6 for 8 data points). (b) Activity ratios, $(^{230}Th)/(^{238}U)$, calculated for analyses of AS3 using the $^{208}Pb/^{206}Pb^*-^{232}ThO^+/^{238}UO^+$ calibration shown in (a). The mean activity ratio is within error of unity, as required by secular equilibrium (MSWD = 1.9 for 14 data points).

and ^{238}U should be equal ($(^{230}Th)/(^{238}U) = 1$). Measured $^{230}Th^{16}O^+/^{238}U^{16}O^+$ ratios exhibit a total range of 13% and yield a weighted average for $(^{230}Th)/(^{238}U) = 1.011 \pm 0.014$ (2σ; Fig. 2). A lack of systematic variation in $^{230}Th^{16}O^+/^{238}U^{16}O^+$ over a more than 20-fold range of $^{238}U^{16}O^+$ intensity indicates that the $^{230}Th^{16}O^+$ peak has been correctly identified, all molecular interferences have been mass resolved, and the background has been appropriately subtracted. The mean square of the weighted deviates (MSWD) for these data (1.9) is within 95% confidence interval for that expected from the in-run statistics [34], albeit at the upper limit. This may indicate that there is a small additional source of scatter besides that due to ion counting.

4. Results

Zircons from the coarsely porphyritic lavas are euhedral, occur principally as isolated grains or in glomerocrysts with Fe–Ti oxides, and often contain inclusions of apatite and Fe–Ti oxides. The largest size fraction zircons from each lava were analyzed (Table 1); those from the South Deadman Dome rhyolite are somewhat larger on average than those from the Deer Mountain lava. Most were heavily abraded by polishing during preparation of the grain mount, which enhanced the likelihood that their cores were exposed. Analyses averaged 30 min and consisted of 120 ratio measurements; every third or fourth analysis was of the AS3 zircon standard. U and Th concentrations were not explicitly determined but UO^+ beam intensities were 2–3 times greater than those of the AS3 zircon standard. Accordingly, U concentrations are probably ~400–800 ppm, similar to that of zircon in the least differentiated Bishop Tuff [2].

Whole-rock analyses of the Deer Mountain and South Deadman Dome coarsely porphyritic rhyolites (Table 1) show that they have similar $(^{230}Th)/(^{232}Th)$ (activity ratio) but that the Deer Mountain rhyolite has a somewhat higher $(^{238}U)/(^{232}Th)$, possibly due to secondary U enrichment. The zircons have uniformly higher $(^{230}Th)/(^{232}Th)$ ratios than the whole rocks (Table 1). The more than six-fold range in this ratio exhibited by the zircons is strongly correlated with $(^{238}U)/(^{232}Th)$, as expected due to ^{230}Th in-growth in response to an excess of ^{238}U. On the other hand, the duration of in situ decay has not been long enough for the majority of the zircons to attain secular equilibrium; most have $(^{230}Th)/(^{238}U) < 1$. Some enrichment in ^{230}Th relative to the whole rock could have been anticipated for the Deer Mountain zircons, as a result of in situ decay of ^{238}U since eruption at 115 ka. For the South Deadman Dome zircons, ^{230}Th enrichment must indicate chemical isolation from the magma for a significant period of time.

To quantify the age significance of $(^{230}Th)/(^{238}U)$, model ages have been calculated relative to the isotopic characteristics of the whole rocks (Table 1; Fig. 3); reported uncertainties are 1σ. Measured whole-rock ratios are quite precise but even an uncertainty of 10% in the magmatic evolution of these ratios has only an ~1% effect on the calculated ages. Because the uncertainty associated with the Th/U correction factor is a systematic one, it has not been propagated into the uncertainties reported in Table 1 and Fig. 3 so that relative differences in model ages will be more apparent. Some general features of the zircon model ages are notable. For the most part, they do not correlate with the $(^{238}U)/(^{232}Th)$ ratio of an analysis (Fig. 3). Duplicate analyses of individual grains give statistically indistinguishable ages, although variations in Th concentrations may have inhibited somewhat the ability to detect younger ages. The diameter of areas sputtered by the ion beam corresponded to 25–50% of the short radial dimensions of the Long Valley zircons; this, coupled with small pits and fractures in the zircons, made it impractical to obtain radial core–rim traverses of the grains.

Model ages for zircons from South Deadman Dome (92LV08) cluster around an age of ~200 ka (Fig. 3), significantly older than the age of eruption (0.6 ka). There is one clear outlier, grain 6, for which the model age is 30 ± 3 ka. This age is similar to ^{230}Th–^{238}U ages for allanite-bearing amphibole (19 ± 12 ka: [9]; 36 ± 2 ka: [35]) from coarsely porphyritic lavas from South Deadman Dome and may indicate an episode of magma cooling. Exclusive of this young zircon, the weighted mean of the two-point zircon–whole-rock isochrons yields an age of 218^{+10}_{-9} ka and an MSWD of 3.3 (Table 2). The uncertainties

and scatter in the slopes of the isochrons were evaluated because, as opposed to the model ages, the errors on these are symmetrical. Two analyses of a second zircon, grain 9, yield ages that are within error of one another, one of which (spot 1) is not within 2σ of the weighted mean. Notably, the model ages for this zircon are within error of the age of eruption of the Deer Mountain rhyolite. If this zircon is also excluded from the mean age, the weighted mean of the two-point isochrons yields a model age of 229^{+12}_{-11} ka (MSWD = 1.3; Table 2).

Like the South Deadman Dome rhyolite, the distribution of zircon model ages for the Deer Mountain rhyolite (92LV05) shows a pronounced peak at ~ 200 ka, but more tailing to younger ages is evident (Fig. 3). Significantly, none of the zircon model ages is younger than the eruption age, further indicating that the measurement technique is accurate within the stated statistical uncertainties. The mean age for 19 spot analyses of 15 zircons, weighted by errors on isochron slopes, is 224 ± 7 ka (Table 2). The MSWD of 8.7 is considerably greater than would be expected if the model ages represented a single population [34]. This should not be surprising given that four of the model ages are within 2σ of the eruption age (115 ka), which is almost 100 ka younger than the mean age.

To evaluate the effect that multiple populations might have on the mean age of the zircons, outliers were sequentially eliminated until the MSWD of the remaining ages was within the range expected at the 95% probability limit [34]. This approach assumes that the in-run errors are representative of the analytical uncertainties. A MSWD of 1.9 and a mean age of 233^{+9}_{-8} ka was obtained after exclusion of 4 spots. The points excluded represent three of the youngest ages (including the two of grain 27) and the oldest (spot 1 of grain 9). Because the second oldest age was also obtained on grain 9, it may that this grain represents an earlier episode of zircon growth than that sampled by the majority of the zircons. If this model age is also excluded, the resulting mean age is only slightly younger, 226^{+9}_{-8} (Table 2). In either case, all but one (spot 1 of grain 2) of the remaining model ages are within 2σ of the mean age (Fig. 3). The three young Deer Mountain zircons have very similar Th/U and yield a mean age (127^{+7}_{-6} ka; MSWD = 1.3) that is similar to that obtained from K–Ar analyses of sanidine [6]. The zircon domains represented by these analyses appear to have grown close to the time of eruption.

5. What do zircon model ages date?

The first-order result of our ion microprobe analyses is that most of the model ages for Deer Mountain and South Deadman dome zircons are considerably older than the age of eruption: only a minority of the zircons, from Deer Mountain, appear to have nucle-

Table 2
Mean model ages and zircon saturation temperatures

	Mean age (ka)	Relative error (±ka)	Absolute error (±ka)	MSWD	SiO_2 (wt%)	Zr (ppm)	T (°C)
South Deadman Dome							
all zircon data (n = 14)	208	9/8	19/17	60	71.72	222	805 ± 8
without gr6sp1	218	10/9	23/18	3.3			
without gr6sp1, gr9sp1&2	229	12/11	25/20	1.3			
Deer Mountain							
all zircon data (n = 18)	224	7/7	17/15	8.7	72.26	193	795
without 2gr1sp1, 2gr9sp1, 2gr27sp1&2	233	9/8	21/17	1.9			
without 2gr1sp1, 2gr9sp1&2, 2gr27sp1&2	226	9/8	20/16	1.4			

Mean ages are calculated from individual zircon model ages. Note that progressive elimination of outliers to reduce the mean square of the weighted deviates (MSWD) to within 95% probability of that from analytical uncertainty [34] has little effect on the mean age. See text for details and Fig. 3 for illustration. Absolute errors include 1σ uncertainties in the Th/U correction factor and the background correction. Temperatures for zircon saturation [4] are based on major element and Zr contents [9,18]. Errors reflect uncertainties from range in reported Zr contents; note that uncertainties in temperature calibration are not included.

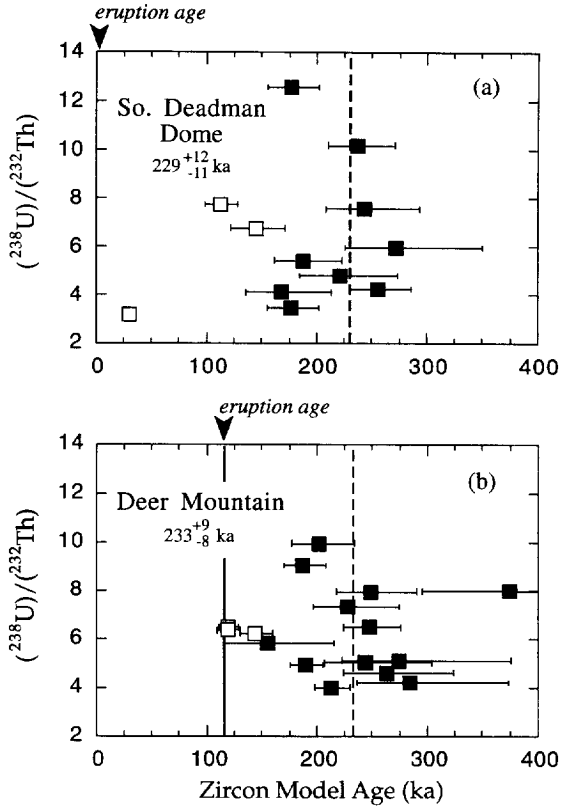

Fig. 3. $(^{238}U)/(^{232}Th)$ (activity ratios) plotted against zircon model ages for (a) the South Deadman Dome rhyolite and (b) the Deer Mountain rhyolite. Errors are 1σ. A weighted mean age, calculated for those samples indicated by filled symbols, is shown by the dashed line in each diagram (see text and Table 2 for details). In (a), gr7sp1 and gr23sp1 are not shown because of large errors; both are included in the weighted mean age. In (b), the two ages for gr9 plot off the diagram and have large errors; gr9sp1 is not included in the weighted mean age.

ated and grown during the undercooling that must have accompanied eruption (Fig. 3). On the other hand, the fact that essentially none of the zircons are in U–Th secular equilibrium shows that the zircons are not simply xenocrysts that have been incorporated unmodified from basement rocks.

Model ages older than that for eruption may date the timing of zircon crystallization but only if the zircons did not subsequently exchange Th with the lower $^{230}Th/^{232}Th$ of the magma, and if U/Th variations within the zircons were not modified after crystallization. Recent experimental evidence [3] shows that U and Th diffusion in zircon is quite slow (Fig. 4). At relevant magmatic temperatures, diffusive Th and U exchange within zircon over the time interval for which $^{230}Th-^{238}U$ disequilibrium might be detected (< 300 ka) can occur only at angstrom length scales. Specific to the rhyolites studied here, where temperatures suggested by mineral equilibria are $\leq 850°C$, $> 5\%$ modification of $^{230}Th-^{238}U$ disequilibria other than by in situ decay could have occurred only between domains that are $< 10^{-5}$ of that sampled by the ion microprobe analyses (Fig. 4). Thus, model ages that cluster around 230 ka (Fig. 3) must date the onset of extensive zircon nucleation and growth. Once clear outliers are excluded, MSWD values of less than 2 are obtained from the scatter in these ages (Table 2), suggesting that the distribution of ages may be largely analytical rather than geological [34].

The older Deer Mountain rhyolite is somewhat more evolved than the much younger, coarsely porphyritic Inyo dome rhyolite but the two can be related by differentiation of the observed crystalline assemblage [9]. The close chemical and textural affinities between the two lavas are reinforced by the general similarity between their present-day

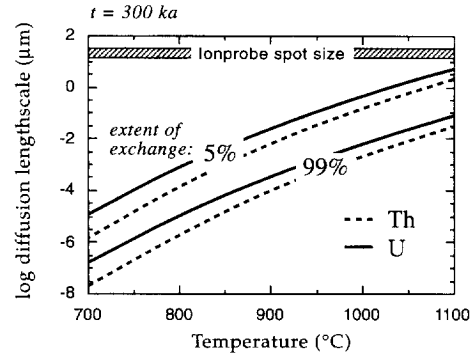

Fig. 4. Characteristic diffusion length scale as a function of temperature for $t = 300$ ka, the maximum time over which $^{230}Th/^{238}U$ disequilibrium is detectable. Diffusion parameters from Cherniak et al. (submitted). Curves for Th and U diffusion are shown for each of two conditions, based on the assumption that compositional layers are plane sheets of thickness a. The dimensionless parameter, Dt/a^2, is equal to $\sim 2\times10^{-4}$ for 5% equilibration and equal to ~ 1 for 99% equilibration [50].

(^{230}Th)/(^{232}Th) and (^{238}U)/(^{232}Th) (Table 1). Further, despite erupting more than 100 ka apart, indistinguishable mean zircon model ages for the two lavas show that they shared a common interval of undercooling and zircon growth; this similarity is robust even though multiple zircon populations are present (Table 2). This concordance between the mean zircon ages, despite differences in crystal sizes and eruption ages, also tends to confirm the expectation that solid-state diffusion has a negligible effect on ^{230}Th/^{238}U disequilibria. It seems likely, therefore, that the coarsely porphyritic Inyo dome lavas did not differentiate from a common mafic magma after eruption of Deer Mountain but, rather, that the two lavas shared a common silicic magma body at least 230 ka ago.

6. Retentivity of zircon by evolved magmas

Given that crystallization ages for the majority of the analyzed zircons predate eruption by more than 100 ka, it appears that zircons may be retained in rhyolitic magmas for protracted periods of time. Zircon aggregates from dacitic lavas in Japan [1,36] also have significantly (20–120 ka) older ^{230}Th ages than ^{14}C and fission track eruption ages, although the significance of these ages is limited by the possibility that xenocrystic grains have been included in the dated population. Zircons of the size analyzed here have Stokes settling velocities on the order of 10^{-9} m/s in a magma with the minimum viscosity estimated for the rhyolites ($\sim 10^4$ Pa s); in a stagnant magma the zircons could have settled several kilometers in 100 ka. Settling rates will be faster for zircons that comprise glomerocrysts with Fe–Ti oxides. In either case, settling velocities are commonly less than those estimated for silicic magma convection, implying that crystals may be kept in suspension by moving magma [37,38]. The importance of convective entrainment can be evaluated by reference to Fig. 5, wherein the major controls on the absolute and relative retentivity of zircon and other phenocrysts present in the Long Valley rhyolites are compared. The rate of crystal settling relative to that of convection has been calculated for a temperature contrast of only 1°C; increasing this value will have the effect of decreasing the relative rate of settling,

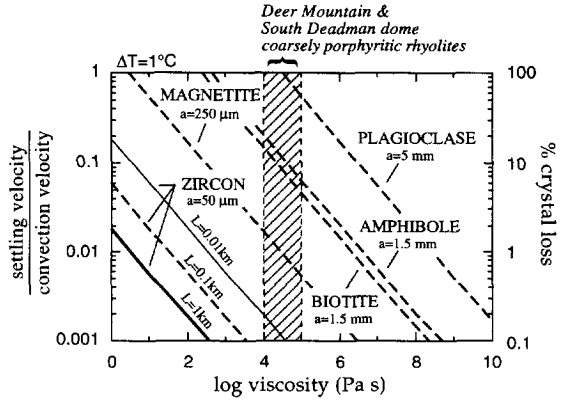

Fig. 5. Ratio of settling to convective velocity for representative phenocrysts with respect to magma viscosity. Right-hand side shows probability of crystal loss, after [38]. The probability that crystals will be lost from a convecting melt is based on the relative magnitude of settling velocities to the rate of convection overturn as a measure of crystal entrainment in the melt. A spherical grain geometry is assumed. A factor of n increase in crystal radius, a, is equivalent to an n^4 decrease in L, the characteristic length scale of the temperature contrast (equal to 1°C in this figure). A minimum viscosity of 10^4 Pa s was estimated from the composition of glass in the coarsely porphyritic Inyo dome lavas [9] using the calibration of [40]. This estimate assumes a maximum water content ($\sim$ 7.5 wt%; [51]) at the conditions of mineral equilibrium (800°C, $\sim$ 2 kbar; [22]) and that the effect of 25% phenocryst content can be estimated by the Einstein–Roscoe formula. Magma rheology is assumed to be Newtonian; non-Newtonian rheologies may help to suspend crystals in magma.

and therefore decreasing the probability of crystal loss at a given viscosity. Comparisons between the representative minerals show that crystal size is a more important determinant of the separation probability than is the magnitude of the density contrast between mineral and magma ($\Delta\rho$) or the characteristic length scale of the thermal contrast (L). For example, biotite and plagioclase have similar values of $\Delta\rho$ but the much larger plagioclase has a significantly greater probability of separation, while amphibole and biotite, which are similar in size but have different values of $\Delta\rho$, have comparable separation probabilities. Zircon, which has one of the higher densities of the phases illustrated, has the lowest probability of settling because of its small size. Thus, zircons are more likely to be retained than major phenocryst phases, except where they are included in those phases, even when conditions are not con-

ducive to convection. Moreover, isolated zircon grains should be strongly retained in magmas with viscosities of $> 10^3$ Pa s, and viscosities of this magnitude characterize virtually all intermediate and silicic magmas at temperatures of zircon stability [39,40].

7. Temperature of zircon crystallization

Experimental determinations of zircon solubility in metaluminous magmas [4,5] permit an estimate of the temperature at which zircon began to crystallize. Considered together with the age of crystallization and the consequences of zircon dissolution rates, aspects of the thermal evolution of the magma chamber can be delimited. For the Deer Mountain and South Deadman rhyolites, zircon saturation temperatures are approximately 795°C and 805 ± 8°C, respectively (Table 2). Although probably insignificant at this composition and temperature, differential separation of the major phenocryst phases following initial zircon saturation (cf. Fig. 5) would tend to cause saturation temperatures to be overestimated somewhat. Zircon saturation temperatures for the coarsely porphyritic Inyo dome lavas are remarkably similar to those obtained from Fe–Ti oxides (809 ± 4°C; [22]). This is particularly notable in view of evidence for co-crystallization of these phases. Temperatures of ~ 800°C are also consistent with experimental constraints on the conditions at which the observed minerals coexist [23,24].

At ~ 800°C, zircon can dissolve fairly rapidly in hydrous melts [5]. A direct consequence of this is that the ages obtained for the majority of zircons in this study almost certainly reflect the last time their host magma(s) cooled through this temperature. Had these magmas, which probably contained > 4 wt.% water, become undersaturated with respect to Zr by, for example, an increase in temperature, the zircons we analyzed would have dissolved in ≤ 1000 years, or < 1% of their apparent residence times. Given the clustering of ages around 230 ka, magma responsible for the South Deadman and Deer Mountain lavas probably has not been at temperatures of > 815°C for periods of longer than 1 ka in the last 200 ka.

8. Evolution of young rhyolites associated with the Long Valley magmatic system

In view of the small volume of the South Deadman Dome and Deer Mountain eruptions (< 1 km^3), intruded magmas of this size might be expected to cool rapidly (< 10 ka; [41,42]), as a result of heat loss to cold upper crustal wallrocks. For this reason, rather than reflecting cooling of a long-lived magma reservoir to the temperature of zircon saturation, it might be supposed that the Th isotope ages reflect near- or complete solidification of intruded magmas; the resulting leucogranites could have subsequently remelted to form the coarsely porphyritic rhyolites (cf. [43,44]). Although we believe that the chemical affinities between rhyolites erupted more 100 ka apart and the euhedral shapes of the zircon contained by them are more easily reconciled with residence in a long-lived, chemically zoned magma reservoir, the overriding issue is the thermal evolution of late Quaternary magmatism along the western margin of Long Valley Caldera. To maintain even near-solidus temperatures in silicic magma systems for periods much longer than 10 ka, either the volume of magma must be very large [41] or there must be an additional heat source. This type of thermal influx could be provided by intrusion of mafic magma [45]. These two effects are complementary because differentiation of intruded mafic magma can contribute volumetrically to the accumulation of evolved magma. Mafic intrusions into the crust can also induce fusion of the basement rocks, as well as remelting of the products of earlier phases of differentiation [46]. If silicic magma, residual after earlier phases of post-caldera volcanism, contributed to the incipient magma chamber, the absence of a zircon population inherited from it must indicate that they dissolved; as we have discussed, zircon dissolution rates are relatively rapid in these magmas. Moreover, if the rhyolites reflect accumulations from convective (e.g., sidewall) fractionation [37,47,48] or repeated episodes of deep crustal melting [46], that portion of the silicic system tapped by these rhyolites has been effectively isolated from these processes for the past 200 ka, analogous to portions of other silicic magma reservoirs [14,16].

The oldest exposed lava in the western moat may be a 228 ± 82 ka trachyandesite [6] but basalts ob-

tained by drilling in the western caldera have ages that suggest that mafic volcanism may have begun as early as 400 ka [19]. It seems likely, therefore, that the coarsely porphyritic rhyolites studied here were generated near the onset of magmatic activity in the western moat and represent a more recent phase of differentiation beneath Long Valley Caldera. At rates of magma generation like those of Long Valley precaldera and syncaldera rhyolites, as well as other evolved magmas [14,16,49], > 20 km^3 of intermediate to silicic magma could have been produced beneath the western portion of the Long Valley caldera system during the past 200 ka. If this magma was fluxed by at least an equivalent amount of mafic magma, a magma chamber could have been thermally stabilized at the upper crustal depths inferred for the Long Valley magma chamber [45]. Notably, a tabular zone, at depths of 7 to 11 km, with a negative velocity perturbation of 30%, occurs just to the south of Deer Mountain [25], the magma from which could have been drawn hydraulically into the conduit during eruption of the southernmost Inyo domes.

Mafic volcanism was abundant in the western moat of Long Valley caldera between 160 and 60 ka [6,8] and associated intruded magmas would have thermally fluxed the resident silicic magma reservoir. In view of this, the thermal evolution of the coarsely porphyritic magmas might be considerably more variable than simply asymptotically approaching the temperature of the enclosing country rocks. Our results show, however, that attendant thermal perturbations did not cause the temperature of these porphyritic magmas to exceed 815°C for any significant period of time after 200 ka, suggesting that the temperature oscillations were damped by latent heat effects. On the other hand, the greater phenocryst content and zircon size of the younger lava is probably not entirely attributable to progressive solidification of the magma body (cf. [9]), given the general lack of evidence for zircon growth in the time interval after eruption of the Deer Mountain rhyolite. The similarity between the youngest zircon age from South Deadman dome and ages previously obtained on allanite-bearing amphibole may offer some evidence for protracted cooling, however. By analogy to the Bishop Tuff, where allanite appears only in the lower temperature magmas, the younger ages may indicate recent thermal decay of the magma reservoir, as might be anticipated from the general absence of volcanism within the western caldera since 50 ka ago.

9. Conclusions

Our results substantiate several important properties of zircon that should permit Th isotope dating of zircon to shed light on the temporal evolution of magmas: (1) Th and U diffusion is quite slow in zircon, even at magmatic temperatures, indicating that $^{238}U-^{230}Th$ disequilibrium will retain the age of zircon crystallization; (2) zircon may remain suspended in the convecting portions of magmas from which it crystallizes; and (3) crystallization ages date cooling of a magma to its zircon saturation temperature, even when the zircons have long magmatic residence times. In those instances where zircon crystallizes well before eruption, the residence time and thermal evolution of its host magma can be constrained.

Specific to the 115 ka Deer Mountain and the 0.6 ka coarsely porphyritic Inyo Dome rhyolites from the western margin of the Long Valley Caldera, only limited zircon growth occurred near the time of eruption. Most zircon growth occurred more than 100 ka before the first of the two eruptions, as indicated by the strong clustering of zircon ages around 230 ka. This concordance, as well as the similarity in whole-rock Th isotope characteristics, corroborates the co-magmatic origin of these two rhyolites inferred by others [8,9]. Accordingly, the coarsely porphyritic Inyo Dome lava tapped the same magma body from which the Deer Mountain lava erupted more than 100 ka before. Whole-rock Zr contents imply temperatures of 795–810°C for zircon saturation, showing that the magma cooled to < 815°C more than 200 ka ago. It seems likely that supersolidus conditions were maintained by the regular influx and differentiation of mafic magma, resulting in the large volume of low velocity material inferred from seismic data to underlie the western moat of the Long Valley caldera.

Acknowledgements

The comments and insights of Alex Halliday, Trevor Ireland, and particularly Gail Mahood are

gratefully acknowledged. This work was supported by NSF EAR9509641 and EAR9418323 and by a UCLA Academic Senate grant to MRR. Gabrielle Littman is thanked for her zircon separations. A White Mountain Research Fellowship enabled MRR to undertake this study. *[FA]*

References

[1] T. Fukuoka, K. Kigoshi, Discordant Io-ages and the uranium and thorium distribution between zircon and host rocks, Geochem. J. 8 (1974) 117–122.

[2] G. Mahood, W. Hildreth, Large partition coefficients for trace elements in high silica rhyolites, Geochim. Cosmochim. Acta 47 (1983) 11–30.

[3] D.J. Cherniak, J.M. Hanchar, E.B. Watson, Diffusion of tetravalent cations in zircon, Contrib. Mineral. Petrol., submitted.

[4] E.B. Watson, T.M. Harrison, Zircon saturation revisited: Temperature and composition effects in a variety of crustal magma types, Earth Planet. Sci. Lett. 64 (1983).

[5] T.M. Harrison, E.B. Watson, Kinetics of zircon dissolution and zirconium diffusion in granitic melts of variable water content, Contrib. Mineral. Petrol. 84 (1983) 66–72.

[6] E.A. Mankinen, C.S. Gromme, G.B. Dalrymple, M.A. Lanphere, R.A. Bailey, Paleomagnetism and K–Ar ages of volcanic rocks from Long Valley Caldera, California, J. Geophys. Res. 91 (1986) 633–652.

[7] C.D. Miller, Holocene eruptions at the Inyo volcanic chain, California: Implications for possible eruptions in Long Valley caldera, Geology 13 (1985) 14–17.

[8] R.A. Bailey, G.B. Dalrymple, M.A. Lanphere, Volcanism, structure and geochronology of Long Valley Caldera, Mono County, California, J. Geophys. Res. 81 (1976) 725–744.

[9] D.E. Sampson, K.L. Cameron, The geochemistry of the Inyo volcanic chain: multiple age systems in the Long Valley region, eastern California, J. Geophys. Res. 92 (1987) 10403–10421.

[10] J.M. Metz, G.A. Mahood, Precursors to the Bishop Tuff eruption: Glass Mountain, Long Valley, California, J. Geophys. Res. 90 (1985) 11121–11126.

[11] M.S. Pringle, M. McWilliams, B.F. Houghton, M.A. Lanphere, C.J.N. Wilson, $^{40}Ar/^{39}Ar$ dating of Quaternary feldspar: Examples from the Taupo Volcanic Zone, New Zealand, Geology 20 (1992) 531–534.

[12] A.N. Halliday, G.A. Mahood, P. Holden, J.M. Metz, T.J. Dempster, J.P. Davidson, Evidence for long residence times of rhyolitic magma in the Long Valley magmatic system: the isotopic record in precaldera lavas of Glass Mountain, Earth Planet. Sci. Lett. 94 (1989) 274–290.

[13] J.N. Christensen, D.J. DePaolo, Time scales of large volume silicic magma systems: Sr isotopic systematics of phenocrysts and glass from the Bishop Tuff, Long Valley, California, Contrib. Mineral. Petrol. 113 (1993) 100–114.

[14] G.R. Davies, A.N. Halliday, G.A. Mahood, C.M. Hall, Isotopic constraints on the production rates, crystallisation histories and residence times of pre-caldera silicic magmas, Long Valley, California, Earth Planet. Sci. Lett. 125 (1994) 17–37.

[15] P. Van den Bogaard, C. Schirnick, $^{40}Ar/^{39}Ar$ laser probe ages of Bishop Tuff quartz phenocrysts substantiate long-live silicic magma chamber at Long Valley, United States, Geology 23 (1995) 759–762.

[16] J.N. Christensen, A.N. Halliday, Rb–Sr ages and Nd isotopic compositions of melt inclusions from the Bishop Tuff and the generation of silicic magma, Earth Planet. Sci. Lett. 144 (1996) 547–561.

[17] R.A. Bailey, Geologic map of the Long Valley caldera, Mono–Inyo Craters volcanic chain, and vicinity, Eastern California, Misc. Invest. Ser. Map I-1933, 1989.

[18] J.C. Eichelberger, T.A. Vogel, L.W. Younker, C.D. Miller, G.H. Heikan, K.H. Wohletz, Structure and stratigraphy beneath a young phreatic vent: South Inyo Crater, Long Valley Caldera, California, J. Geophys. Res. 93 (1988) 13208–13220.

[19] T.A. Vogel, T.B. Woodburne, J.C. Eichelberger, P.W. Layer, Chemical evolution and periodic eruption of mafic lava flows in the west moat of Long Valley Caldera, California, J. Geophys. Res. 99 (1994) 19829–19842.

[20] D.E. Sampson, Textural heterogeneities and vent area structures in the 600-year-old lavas of the Inyo volcanic chain, eastern California, Geol. Soc. Am. Spec. Pap. 212 (1987) 89–101.

[21] S. Blake, J.H. Fink, The dynamics of magma withdrawal from a density stratified dyke, Earth Planet. Sci. Lett. 85 (1987) 516–524.

[22] T.A. Vogel, J.C. Eichelberger, L.W. Younker, B.C. Schuraytz, J.P. Horkowitz, H.W. Stockman, H.R. Westrich, Petrology and emplacement dynamics of intrusive and extrusive rhyolites of Obsidian Dome, Inyo craters volcanic chain, eastern California, J. Geophys. Res. 94 (1989) 17937–17956.

[23] M.T. Naney, Phase equilibria of rock-forming ferromagnesian silicates in granitic systems, Am. J. Sci. 283 (1983) 993–1033.

[24] R.G. Gibson, M.T. Naney, Textural development of mixed, finely porphyritic silicic volcanic rocks, Inyo Domes, Eastern California, J. Geophys. Res. 97 (1992) 4541–4559.

[25] L.K. Steck, W.A. Prothero Jr., Crustal structure beneath Long Valley caldera from modeling of teleseismic P wave polarizations and Ps converted waves, J. Geophys. Res. 99 (1994) 6881–6898.

[26] P.B. Dawson, J.R. Evans, H.M. Iyer, Teleseismic tomography of the compressional wave velocity structure beneath the Long Valley region, California, J. Geophys. Res. 95 (1990) 11021–11050.

[27] S.F. Carle, Three-dimensional gravity modeling of the geological structure of Long Valley caldera, J. Geophys. Res. 93 (1988) 13237–13250.

[28] J.B. Gill, D.M. Pyle, R.W. Williams, Igneous rocks, in: M. Ivanovich, R.S. Harmon (Eds.), Uranium-series Disequilibrium: Applications to Earth, Marine, and Environmental Sciences, Clarendon Press, Oxford, 1992, pp. 207–258.

[29] M.R. Reid, F.C. Ramos, Chemical dynamics of enriched mantle in the southwestern United States: Thorium isotope evidence, Earth Planet. Sci. Lett. 138 (1996) 67–81.
[30] A.P. Nutman, M.T. Rosing, SHRIMP U–Pb zircon geochronology of the late Archaean Ruinnæsset syenite, Skjoldungen alkaline province, southeast Greenland, Geochim. Cosmochim. Acta 58 (1994) 3515–3518.
[31] L.P. Black, B.L. Gulson, The age of the Mud Tank carbonatite, Strangways Range, Northern Territory, BMR J. Aust. Geol. Geophys. 3 (1978) 227–232.
[32] J.B. Paces, J.D. Miller, U–Pb ages of Duluth complex and related mafic intrusions, northeastern Minnesota: Geochronological insights to physical, petrogenetic, paleomagnetic, and tectonomagmatic processes associated with the 1.1 Ga midcontinent rift system, J. Geophys. Res. 98 (1993) 13997–14013.
[33] X. Quidelleur, M. Grove, O.M. Lovera, T.M. Harrison, A. Yin, F.J. Ryerson, Thermal evolution and slip history of the Renbu Zedong Thrust, southeastern Tibet, J. Geophys. Res. 102 (1997) 2659–2679.
[34] I. Wendt, C. Carl, The statistical distribution of the mean squared weighted deviation, Chem. Geol. (Isot. Geosci. Sect.) 86 (1991) 275–285.
[35] A. Taddeucci, W.S. Broecker, D.L. Thurber, ^{230}Th dating of volcanic rocks, Earth Planet. Sci. Lett. 3 (1967) 338–342.
[36] T. Fukuoka, Ionium dating of acidic volcanic rocks, Geochem. J. 8 (1974) 109–116.
[37] R.S.J. Sparks, H.E. Huppert, J.S. Turner, The fluid dynamics of evolving magma chambers, Philos. Trans. R. Soc. London 310 (1984) 511–534.
[38] B.D. Marsh, M.R. Maxey, On the distribution and separation of crystals in convecting magma, J. Volcanol. Geotherm. Res. 24 (1985) 95–150.
[39] Y. Bottinga, D.F. Weill, The viscosity of magmatic silicate liquids: a model for calculation, Am. J. Si. 272 (1972) 438–475.
[40] H.R. Shaw, Viscosities of magmatic silicate liquids: An empirical method of prediction, Am. J. Sci. 272 (1972) 870–893.
[41] F.J. Spera, J.A. Crisp, Eruption volume, periodicity, and caldera area: Relationships and inferences on development of compositional zonation in silicic magma chambers, J. Volcanol. Geotherm. Res. 11 (1981) 169–187.
[42] H.S. Carslaw, J.C. Jaeger, Conduction of Heat in Solids, Clarendon Press, Oxford, 1959.
[43] R.S.J. Sparks, H.E. Huppert, C.J.N. Wilson, Comment on "Evidence for long residence times of rhyolitic magma in the Long Valley magmatic system: the isotopic record in precaldera lavas of Glass Mountain" by A.N. Halliday, G.A. Mahood, P. Holden, J.M. Metz, T.J. Dempster and J.P. Davidson, Earth Planet. Sci. Lett. 99 (1990) 387–389.
[44] G.A. Mahood, Second reply to comment of R.S.J. Sparks, H.E. Huppert and C.J.N. Wilson on "Evidence for long residence times of rhyolitic magma in the Long Valley magmatic system: the isotopic record in the precaldera lavas of Glass Mountain", Earth Planet. Sci. Lett. 99 (1990) 395–399.
[45] A.H. Lachenbruch, J.H. Sass, R.J. Munroe, T.H.J. Moses, Geothermal setting and simple heat conduction models for the Long Valley caldera, J. Geophys. Res. 81 (1976) 769–784.
[46] H.E. Huppert, R.S.J. Sparks, The generation of granitic magmas by intrusion of basalt into continental crust, J. Petrol. 29 (1988) 599–624.
[47] A.R. McBirney, B.H. Baker, R.H. Nilson, Liquid fractionation. Part I: Basic principles and experimental simulations, J. Volcanol. Geotherm. Res. 24 (1985) 1–24.
[48] R.H. Nilson, A.R. McBirney, B.H. Baker, Liquid fractionation. Part II: Fluid dynamics and quantitative implications for magmatic systems, J. Volcanol. Geotherm. Res. 24 (1985) 25–54.
[49] A.F. Trial, F.J. Spera, Mechanisms for the generation of compositional heterogeneities in magma chambers, Geol. Soc. Am. Bull. 102 (1990) 353–367.
[50] J. Crank, The Mathematics of Diffusion, Oxford Univ. Press, New York, 1975.
[51] O. Paillat, S.C. Elphick, W.L. Brown, The solubility of water in $NaAlSi_3O_8$ melts: A re-examination of Ab–H_2O phase relationships and critical behaviour at high pressures, Contrib. Mineral. Petrol. 112 (1992) 490–500.